

See discussions, stats, and author profiles for this publication at: <https://www.researchgate.net/publication/41415579>

Live-Cell One- and Two-Photon Uncaging of a Far-Red Emitting Acridinone Fluorophore

ARTICLE in JOURNAL OF THE AMERICAN CHEMICAL SOCIETY · FEBRUARY 2010

Impact Factor: 12.11 · DOI: 10.1021/ja9074562 · Source: PubMed

CITATIONS

60

READS

98

13 AUTHORS, INCLUDING:



David Warther

University of California, San Diego

15 PUBLICATIONS 223 CITATIONS

SEE PROFILE



Alexandre Specht

French National Centre for Scientific Resea...

50 PUBLICATIONS 1,123 CITATIONS

SEE PROFILE



Jean-Luc Vonesch

Institut de Génétique et de Biologie Moléc...

79 PUBLICATIONS 4,238 CITATIONS

SEE PROFILE



Jean-François Nicoud

University of Strasbourg

165 PUBLICATIONS 4,469 CITATIONS

SEE PROFILE

Live-Cell One- and Two-Photon Uncaging of a Far-Red Emitting Acridinone Fluorophore

David Warther,[†] Frédéric Bolze,[‡] Jérémie Léonard,[§] Sylvestre Gug,^{†,‡}
 Alexandre Specht,[†] David Puliti,[†] Xiao-Hua Sun,[‡] Pascal Kessler,[‡] Yves Lutz,[‡]
 Jean-Luc Vonesch,[‡] Barbara Winsor,[¶] Jean-François Nicoud,[‡] and
 Maurice Goeldner^{*,†}

Laboratoire de Conception et Application de Molécules Bioactives, UMR 7199 CNRS, Faculté de Pharmacie, Université de Strasbourg, 74 Route du Rhin 67401 Illkirch Cédex, France, Laboratoire de Biophotonique et de Pharmacologie, UMR 7213 CNRS, Faculté de Pharmacie, Université de Strasbourg, France, Institut de Physique et Chimie des Matériaux de Strasbourg, Université de Strasbourg, CNRS UMR 7504, 23 rue du Loess, BP43, 67034 Strasbourg Cédex 2, France, Institut de Génétique et de Biologie Moléculaire et Cellulaire, Imaging Center Technology Platform, 1 rue Laurent Fries, BP 10142, 67404 Illkirch Cédex, France, and Département de Biologie Moléculaire et Cellulaire, UMR 7156 CNRS, Université de Strasbourg, 21 rue Descartes, 67084 Strasbourg Cédex, France

Received September 3, 2009; E-mail: goeldner@unistra.fr

Abstract: Total synthesis and photophysical properties of PENB-DDAO, a photoactivatable 1,3-dichloro-9,9-dimethyl-9H-acridin-2(7)-one (DDAO) derivative of a far-red emitting fluorophore, are described. The photoremovable group of the DDAO phenolic function comprises a donor/acceptor biphenyl platform which allows an efficient ($\geq 95\%$) and rapid ($< 15 \mu\text{s}$ time-range) release of the fluorescent signal and displays remarkable two-photon uncaging cross sections ($\delta_a \cdot \Phi_u = 3.7 \text{ GM}$ at 740 nm). PENB-DDAO is cell permeable as demonstrated by the triggering of cytoplasmic red fluorescent signal in HeLa cells after one-photon irradiation (λ_{exc} around 360 nm) or by the generation of a red fluorescent signal in a delineated area of a single cell after two-photon photoactivation ($\lambda_{\text{exc}} = 770 \text{ nm}$).

Introduction

The search for red-emitting fluorescent labels that are controlled in time and space has become a major challenge in cellular imaging. Most efforts have been put on developing photoactivatable fluorescent protein tags for use as protein fusions,¹ focusing more recently on red-emitting genetically encoded proteins² as powerful tools for live cell imaging. However, in many cases the development of small photoactivatable fluorophore molecules (caged fluorophores) are of particular interest for intracellular protein dynamics.³ These probes allow a rapid and efficient light-induced fluorescence enhancement, leading to spatiotemporal control of the luminescent signal in biological systems. While photoactivated fluorescence is well described in the chemical literature,⁴ biological applications require specific photophysical properties. The phenolic group of fluorescein was first targeted in this respect,⁵ subsequent extensions include rhodamine,⁶ Q-rhodamine,⁷ and

resorufin,⁷ using *o*-nitrobenzyl (*o*-NB) derivatives as caging groups. Similar *o*-NB caging groups were used on fluorescein derivatives with improved fluorescent properties (TokyoGreen).⁸ Hydroxycoumarin derivatives were modified using either *o*-NB⁹ or *o*-nitrophenethyl (DMNPB)¹⁰ derived caging groups resulting in enhanced two-photon uncaging sensitivity. A different photochemical reaction was recently described on a masked push–pull fluorophore by photochemical conversion of a nonfluorescent aromatic azido-DCDHF label into the corresponding fluorescent anilino derivative.¹¹ Alternative approaches described alcohol and carboxylic acid uncaging systems with concomitant release of fluorescent coumarin¹² and xanthone,¹³ respectively, as reporter molecules.

[†] UMR 7199 CNRS, Université de Strasbourg.

[‡] UMR 7213 CNRS, Université de Strasbourg.

[§] UMR 7504 CNRS, Université de Strasbourg.

[‡] Imaging Center Technology Platform.

[¶] UMR 7156 CNRS, Université de Strasbourg.

- (1) Shaner, N. C.; Patterson, G. H.; Davidson, M. W. *J. Cell Sci.* **2007**, *120*, 4247–4260.
- (2) Subach, F. V.; Patterson, G. H.; Manley, S.; Gillette, J. M.; Lippincott-Schwartz, J.; Verhusha, V. V. *Nat. Methods* **2008**, *6*, 153–159.
- (3) Theriot, J. A.; Mitchison, T. J. *Nature* **1991**, *351*, 126–131.
- (4) Zweig, A. *Pure Appl. Chem.* **1973**, *33*, 389–410.

- (5) Krafft, G. A.; Sutton, W. R.; Cummings, R. T. *J. Am. Chem. Soc.* **1988**, *110*, 301–303.
- (6) Ottl, J.; Gabriel, D.; Marriott, G. *Bioconjugate Chem.* **1998**, *9*, 143–151.
- (7) Mitchison, T. J.; Sawin, K. E.; Theriot, J. A.; Gee, K.; Mallavaparu, A. *Methods Enzymol.* **1998**, *291*, 63–78.
- (8) Kobayashi, T.; Urano, Y.; Kamiya, M.; Ueno, T.; Kojima, H.; Nagano, T. *J. Am. Chem. Soc.* **2007**, *129*, 6696–6697.
- (9) Zhao, Y.; Zheng, Q.; Dakin, K.; Xu, K.; Martinez, M. L.; Li, W.-H. *J. Am. Chem. Soc.* **2004**, *126*, 4653–4663.
- (10) Orange, C.; Specht, A.; Puliti, D.; Sakr, E.; Furuta, T.; Winsor, B.; Goeldner, M. *Chem. Commun.* **2008**, 1217–1219.
- (11) Lord, S. J.; Conley, N. R.; Lee, H. D.; Samuel, R.; Liu, N.; Twieg, R. J.; Moerner, W. E. *J. Am. Chem. Soc.* **2008**, *130*, 9204–9205.
- (12) Gagey, N.; Emond, M.; Neveu, P.; Benbrahim, C.; Goetz, B.; Aujard, I.; Baudin, J.-B.; Jullien, L. *Org. Lett.* **2008**, *10*, 2341–2344.
- (13) Blake, J. A.; Lukeman, M.; Scaiano, J. C. *J. Am. Chem. Soc.* **2009**, *131*, 4127–4135.

The development of photoremovable protecting groups that are susceptible to rapidly and efficiently release a fluorescent probe inside a cell requires excitation wavelengths in the near-UV or visible regions,¹⁴ to minimize cell damages compared to UV excitation. Alternatively, caging groups that are responsive to two-photon excitation (IR excitation) would not only overcome the problems related to cell damages but also to cellular autofluorescence. To date, 7-hydroxycoumarin-3-carboxamide derivatives are the only caged fluorophores for which two-photon uncaging excitation has been used,^{9,10} leading to two-photon uncaging cross sections $\delta_a \cdot \Phi_u \leq 0.6$ Goeppert-Mayer (GM, 1 GM = 10^{-50} cm⁴·s·photon⁻¹·molecule⁻¹) at 740 nm for the 1-(2-nitrophenyl)ethyl cage (where δ_a is the two-photon absorption cross section and Φ_u is the uncaging quantum yield).¹⁵ Another important constraint concerning the development of caged fluorophores is the selection of probes displaying high brightness at long wavelengths (>600 nm) and that are available in large quantities to allow convenient syntheses. Most long wavelength-emitting fluorophores possess rather complex structures¹⁶ and do not necessarily contain a chemical function modifiable by a photoactivatable group to abolish the fluorescence. Resorufin derivatives were the only red-emitting probes displaying a simple backbone and possessing an appropriate phenolic function for caging.⁶ Unfortunately these derivatives are extremely prone to bleaching, preventing reliable time-dependent fluorescence measurements.

Red-emitting caged fluorophores which can be efficiently uncaged by two-photon photolysis remain highly desirable tools. These probes are best adapted for live-cell imaging, limiting toxicity, and autofluorescence background, as well as allowing a remarkable increase in the spatial resolution of the fluorescent signal. Here we report the synthesis, together with the chemical and photophysical properties, of a caged 1,3-dichloro-9,9-dimethyl-9H-acridin-2(7)-one (DDAO) derivative,¹⁷ a far-red emitting fluorophore ($\lambda_{em} = 658$ nm) using a 3-(2-propyl)-4'-tris-ethoxy(methoxy)-4-nitrobiphenyl (PENB) group as the phenolic caging moiety. This caged fluorophore, besides allowing a rapid and efficient release of the fluorescent signal, displayed remarkable two-photon uncaging cross sections ($\delta_a \cdot \Phi_u = 3.7$ GM at 740 nm).

Experimental Section

All chemicals and reagents were purchased from Alfa Aesar, Acros, Sigma Aldrich, or TCI and used without any further purification. Solvents were purified and dried by standard procedures (see Supporting Information). TLCs were run on Merck precoated aluminum plates (Si 60 F254). Column chromatographies were run on Merck Silica Gel (60–120 mesh). ¹H and ¹³C spectra were performed with a 300 MHz Bruker Advance 300, 200 MHz Bruker Advance 200, or Ultrashield plus 400 MHz Advance III 400 instrument in CDCl₃ (internal standard 7.24 ppm for ¹H and 77 ppm for ¹³C spectra) or DMSO-*d*₆ (internal standard 2.5 ppm for ¹H and 39.5 ppm for ¹³C spectra).

Mass spectra were recorded with a Agilent QToF 4 GHz introdirect electrospray. Analysis HPLC methods 1 and 2 and purification HPLC method 3 are described in the Supporting

Information. UV–visible spectra were performed on a Uvikon XL from BioTek Instruments and monitored with the software LabPower 3000. Fluorescence spectra were performed on a Fluoromax 4 from Horiba JobinYvon and monitored with the software Fluorescence. 1,3-Dichloro-9,9-dimethyl-9H-acridin-2(7)-one (DDAO 1) was prepared as described by Corey et al.,¹⁷ 2-ethyl-4-iodo-1-nitrobenzene and 2-(5-iodo-2-nitrophenyl)-propan-1-ol were prepared as described by Bühler et al.¹⁸ and by Walbert et al.,¹⁹ respectively.

4-Tris-ethoxy(methoxy)-1-bromo-benzene (5). NaH (1.6 g; 36.6 mmol) was slowly added to a solution of *p*-bromophenol (3.0 g; 13.6 mmol) in dry THF (50 mL), and the mixture was heated to reflux during 1 h. Tris-ethoxy(methoxy)-*p*-toluenesulfonate (5.6 g; 27.6 mmol) was rapidly added and the solution was refluxed for an additional 12 h. After cooling, the mixture was poured in 100 mL of a 2 M solution of H₂SO₄ and was extracted with CH₂Cl₂. The organic layer was dried on MgSO₄, and solvent was removed under vacuum. Crude product was purified by column chromatography (SiO₂; heptane/AcOEt 70:30 v:v). 4-Tris-ethoxy(methoxy)-1-bromo-benzene was obtained as a slightly yellow oil (4.0 g; 90%).

¹H NMR, CDCl₃, δ (ppm) = 7.5 (d; 2H); 6.65 (d; 2H); 3.8 (m; 2H); 3.7 (m; 2H); 3.6 (m; 4H); 3.5 (m; 4H); 3.3 (s; 2H). ¹³C NMR, CDCl₃, δ (ppm) = 113.90; 129.60; 127.72; 116.85; 71.69; 70.60; 70.49; 70.41; 70.33; 69.03; 67.31; 58.81.

4-Tris-ethoxy(methoxy)phenylboronic Acid (6). 4-Tris-ethoxy(methoxy)-1-bromo-benzene (1.2 g; 3.27 mmol) was suspended in dry THF under argon and cooled to –78 °C. *N*-BuLi (3.43 mL; 1.6 M in hexane) was then dropwise added. Solution was stirred at –78 °C during 30 min. Trimethylborate (500 mg; 4.8 mmol) was added and the mixture was allowed to warm up to room temperature during 12 h. Reaction medium was then hydrolyzed by a 7% HCl solution, extracted with ethyl acetate, and then dried on MgSO₄. The solvent was removed under vacuum and the crude product was used without further purification.

3-(2-Propyl-1-ol)-4'-tris-ethoxy(methoxy)-4-nitrobiphenyl (PENB-OH, 2). 2-(5-Iodo-2-nitrophenyl)propan-1-ol (507 mg; 1.66 mmol) was suspended in dry toluene (30 mL) under argon. Tetrakis triphenylphosphine palladium (200 mg; 0.19 mmol) was then slowly added to the mixture and stirred until it was fully dissolved. Na₂CO₃ in water (20 mL) was then added. The mixture was then heated at 110 °C during 30 min. 4-Tris-ethoxy(methoxy)phenylboronic acid (1 g; 3.29 mmol) was dissolved in ethanol (3 mL) and dropwise added to the mixture. The reaction was stirred at 110 °C and followed by TLC. After reaction, the mixture was cooled to room temperature, diluted with brine, and extracted with ethyl acetate. The organic layer was then washed with water and dried on MgSO₄ and the solvent was removed under vacuum. The crude product was purified on column chromatography (SiO₂; cyclohexane/AcOEt 2/8 v:v). PENB-OH was obtained as a slight yellow viscous oil (320 mg; 46%). ¹H NMR, CDCl₃, δ (ppm) = 7.79 (d; 1H); 7.58 (d; 1H); 7.45 (m; 3H); 6.98 (d; 3H); 4.14 (m; 2H); 3.85 (m; 4H); 3.65 (m; 6H); 3.50 (m; 4H); 3.31 (s; 3H); 1.30 (t; 3H). ¹³C NMR, CDCl₃, δ (ppm) = 159.0; 148.42; 144.86; 138.82; 131.16; 128.06; 125.87; 124.63; 124.57; 114.78; 99.23; 71.51; 70.42; 70.23; 70.12; 69.26; 67.18; 58.29; 36.11; 17.29.

7(2)-{3-(2-Propyl)-4'-tris-ethoxy(methoxy)-4-nitrobiphenyl}-6,8-dichloro-9,9-dimethylacridin-2-one (PENB-DDAO, 3a and 3b). In a dry 10 mL round flask, DDAO (100 mg; 0.325 mmol) and PENB (272 mg; 0.649 mmol) are dissolved in anhydrous benzene under argon.

In a dry 5 mL round flask, triphenylphosphine (255 mg; 0.975 mmol) and diisopropyl azodicarboxylate (192 μ L; 0.975 mmol) are dissolved in anhydrous benzene (1.2 mL) under argon and stirred before being added slowly to the previous mixture. The 5 mL flask

(14) (a) For reviews see: *Dynamic studies in Biology, Phototriggers, Photoswitches and Caged Biomolecules*; Goeldner, M., Givens, R., Eds.; Wiley-VCH: Weinheim, Germany, 2005. (b) Mayer, G.; Heckel, A. *Angew. Chem., Int. Ed.* **2006**, *45*, 4900–4921.

(15) Dakin, K.; Li, W.-H. *Nat. Methods* **2006**, *3*, 959.

(16) For a useful chart see: Lavis, L. D.; Raines, R. T. *ACS Chem. Biol.* **2008**, *3*, 142–155.

(17) Corey, P. F.; Trimmer, R. W.; Biddlecom, W. G. *Angew. Chem., Int. Ed.* **1991**, *103*, 1646–1648.

(18) Bühler, S.; Lagoja, I.; Giegrich, H.; Stengele, K.-P.; Pfeiderer, W. *Helv. Chim. Acta* **2004**, *87*, 620–659.

(19) Walbert, S.; Pfeiderer, W.; Steiner, U. E. *Helv. Chim. Acta* **2001**, *84*, 1601–1611.

is washed with 1.2 mL of anhydrous benzene, which is then dropwise added to the reaction mixture.

This mixture is stirred at room temperature for 5 h under argon. After reaction, the solvent is removed under vacuum. The crude mixture is purified by HPLC (method 3, retention time: 31.35 min.). **3a** and **3b** are obtained as a dark-orange viscous oil, with 60% yields. **3a**: ^1H NMR, DMSO, 300 MHz, δ (ppm) = 7.97 (d, 1H, J = 1.4 Hz); 7.92 (d, 1H, J = 8.7 Hz); 7.76–7.70 (m, 2H); 7.41 (d, 1H, J = 9.8 Hz); 7.07 (d, 2H, J = 9.8 Hz); 6.86 (d, 1H, J = 2 Hz); 6.67 (dd, 1H, J = 9.8 Hz; 1.9 Hz); 4.42 (t, 1H, J = 8.5 Hz); 4.30–4.25 (m, 1H); 4.16–4.13 (m, 3H); 3.90–3.83 (m, 1H); 3.77–3.74 (m, 3H); 3.60–3.50 (m, 8H); 3.43–3.40 (m, 3H); 3.22 (s, 3H); 1.67 (d, 6H, J = 3.1 Hz). ^{13}C NMR, DMSO, 400 MHz, δ (ppm) = 186.81; 159.12; 155.85; 152.52; 152.40; 148.41; 147.80; 144.13; 140.64; 139.59; 137.70; 133.47; 132.06; 131.75; 130.31; 128.47; 128.42; 126.93; 126.07; 125.11; 124.81; 115.02; 77.09; 77.06; 71.23; 69.91; 69.89; 69.75; 69.56; 68.85; 67.29; 57.99; 37.61; 34.52; 27.97; 27.95. HRMS: m/z = 708.1998 (calculated for $\text{C}_{37}\text{H}_{38}\text{Cl}_2\text{N}_2\text{O}_8$: 708.2005). UV: λ_{max} = 390 nm, ϵ = 10000 $\text{M}^{-1}\cdot\text{cm}^{-1}$ in PBS. **3b** was detected on HPLC (retention time = 32.03 min.) but was obtained in too low amounts ($\leq 5\%$) to be identified by NMR.

Spectral Properties. Fluorescence Quantum Yield (Φ_f). Solutions of DDAO in PBS and rhodamine B 20 in acidic ethanol (ethanol with TFA 6% v/v, $\Phi_{\text{rhodamine B}}$ = 0.49) with OD's around 0.2 at 498 nm are precisely measured before being diluted 10-times in their respective solvent. Both DDAO and rhodamine B solutions are excited at 498 nm, and fluorescence emissions are measured from 510 to 800 nm. The emission spectra are corrected by the fluorimeter's software, and the fluorescence curves are integrated (area under the curve = I). The fluorescence quantum yield of DDAO is then calculated according to

$$\Phi_f = \Phi_{\text{Rhodamine B}} \frac{I_{\text{DDAO}} \text{OD}_{\text{Rhodamine B}}}{I_{\text{Rhodamine B}} \text{OD}_{\text{DDAO}}} \quad (1)$$

One-Photon Quantum Yield of Disappearance (Φ_{dis}). The quantum yield for the photoconversion of PENB-DDAO is determined by comparison with the photolysis of PMNB-Glu (Φ_{dis} = 0.1) 21 in phosphate buffer (0.1 mM, pH 7.4) (PB) at 25 °C, which is taken as reference. Solutions of PENB-DDAO and PMNB-Glu are prepared from stock solutions in DMSO and are adjusted to an OD of 0.3 at 315 nm in a acetonitrile/PB (1:1) mixture. A mixture of both solutions (3.5 mL, 1:1) are then exposed to a 1000 W Hg Lamp from Hanovia focused on the entrance slit of a monochromator at 315 (± 0.2 nm). Several 200 μL aliquots are taken at different times: 0, 1, 2, 3.5, 5, and 8 min and are subjected to reversed-phase HPLC (method 2) to determine the extent of the photolytic conversions. The retention times of PENB-DDAO and PMNB-Glu are 32.96 and 20.78 min, respectively. Quantum yields are calculated according to formula 2, by considering the conversions up to 30%, to limit, as much as possible, errors due to undesired light absorption by side products during photolysis (slopes are determined from the graphical representation of the photolytic conversion).

$$\Phi_{\text{dis}} = \Phi_{\text{disPMNB-Glu}} \frac{\text{slope}_{\text{PENB-DDAO}}}{\text{slope}_{\text{PMNB-Glu}}} \quad (2)$$

Ratio of Released DDAO (percent $_{\text{released DDAO}}$). The ratio of released DDAO from irradiated PENB-DDAO is determined by HPLC analysis. A 500 μL portion of a 1.95×10^{-5} M solution of PENB-DDAO in a mixture of acetonitrile/PB (1:1) was irradiated during 30 min at 315 nm to ensure a complete conversion of the starting compound. This mixture was analyzed by HPLC (method

1, retention time: 24.43 min) and compared to the HPLC analysis (method 1) of a 500 μL of a 1.61×10^{-5} M solution of DDAO in PB, taken as a reference (retention time = 24.40 min). The ratio of released DDAO was the calculated according to formula 3 (I = area of the corresponding HPLC peak).

$$\text{percent}_{\text{released DDAO}} = \frac{[\text{DDAO}_{\text{reference}}] I_{\text{released DDAO}}}{[\text{PENB-DDAO}] I_{\text{DDAOREference}}} 100 \quad (3)$$

One-Photon Uncaging Quantum Yield (Φ_u). This quantum yield corresponds to the overall yield of released DDAO after one-photon excitation of PENB-DDAO and is calculated according to

$$\Phi_u = \frac{\Phi_{\text{dis}} \times \text{percent}_{\text{released DDAO}}}{100} \quad (4)$$

Kinetics of the Uncaging Process. The kinetics of the uncaging process was measured by following the fluorescence release. The photolysis of PENB-DDAO 3 in a 100- μL buffer solution is triggered impulsively by the one-photon absorption of a unique, nanosecond, UV laser pulse at 355 nm (~ 30 mJ/cm 2). A light emitting diode (LED) operating around 590 nm continuously excites the fluorescence of the released chromophores while a photomultiplier tube (PMT) monitors the amount of fluorescence collected at wavelengths > 640 nm.

Two-Photon Uncaging Cross-Section at 740 nm. Solutions of PENB-DDAO and PMNB-Glu, taken as a reference (two-photon cross-section of 3.13 GM at 740 nm), 21 are prepared from stock solutions in DMSO and are adjusted to an OD of 0.5 in acetonitrile/PB (1:1 v/v) at 370 nm (740 nm/2). A 100 μL portion of each solution is irradiated during 50 min by mode-locked titanium: sapphire laser, Tsunami, Spectra Physics, 100 fs, 80 MHz) at 740 nm. The measurements were performed at P = 250 mW, in the quadratic dependence range for such chromophore. 21 After irradiation, 80 μL of each solution is analyzed by HPLC (method 1 for PMNB-Glu; retention time, 20.08 min, and method 2 for PENB-DDAO, retention time, 32.96 min). The areas of the peaks are determined and the percent of remaining caged species is reported on a graph. Each result is the mean of at least three independent measurements. The ratio between the slopes determined from the graphical representation of the photolytic conversion allows an estimation of a cross section of 3.7 GM for PENB DDAO (using CouOAc 22 as primary standard, for which the two-photon uncaging action cross section of 1.07 at 740 nm is accurate within a factor of 2).

Two-Photon Cross-Section Measurements by Fluorescence Release Analyses. A 100 μL portion of a solution of PENB-DDAO (OD = 0.05) was irradiated by two-photon excitation at 740, 760, 780, 800, 840, and 900 nm, respectively (same conditions as before) during 45 min at identical laser power. 21 After irradiation, fluorescence of each sample was recorded on a spectrofluorimeter (Fluorolog from Jobin-Yvon). Excitation was performed at 600 nm, and emission was recorded from 610 to 800 nm. The fluorescence curves were integrated (I = area under the curve) and the two-photon cross sections were determined by comparison with the 3.7 GM two-photon cross-section value (determined by HPLC) obtained by excitation at 740 nm, according to

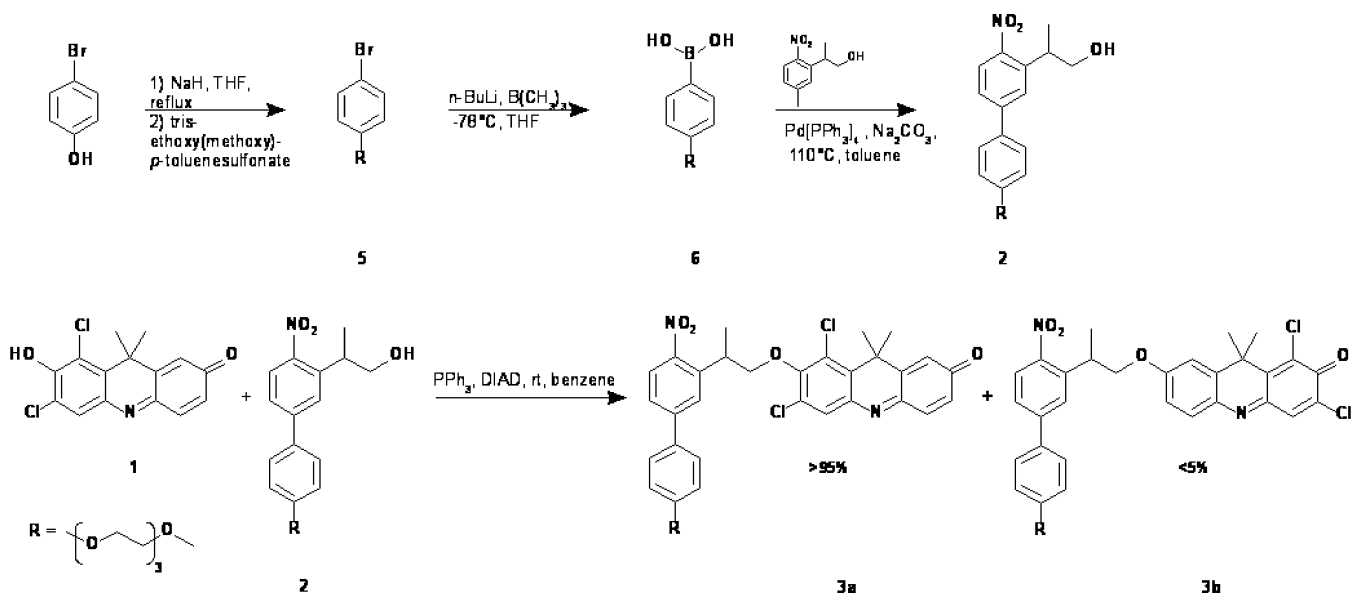
$$\delta_a \cdot \Phi_u = 3.7 \times \frac{I}{I_{740 \text{ nm}}} \quad (5)$$

Cell Imaging. For all experiments HeLa cells were incubated for 30 min with a solution of PENB-DDAO in HBSS (1.95×10^{-5} M) prepared from a stock solution of PENB-DDAO 3 in DMSO

(20) Casey, K. G.; Quitevis, E. L. *J. Phys. Chem.* **1988**, 92, 6590–6594.
(21) Gug, S.; Bolze, F.; Specht, A.; Bourgogne, C.; Goeldner, M.; Nicoud, J.-F. *Angew. Chem., Int. Ed.* **2008**, 47, 9525–9529.

(22) Furuta, T.; Wang, S. S.; Dantzker, J. L.; Dore, T. M.; Bybee, W. J.; Callaway, E. M.; Denk, W.; Tsien, R. Y. *Proc. Natl. Acad. Sci. U.S.A.* **1999**, 96, 1193–1200.

Scheme 1. Synthesis of PENB-OH 2 and PENB-DDAO 3



(1.95×10^{-3} M). Observations were performed with a Water objective Leica HCX PL Apo W Corr Cs NA 1,20 between 10 to 15 s after irradiation. The switch between uncaging with the HBO lamp (340–380 nm) or one (405 nm)- or two-photon laser (770 nm), and excitation for imaging at 633 nm, was done manually, generating a slight variability in the time-delays. Pre- and postuncaging acquisitions were performed in the transmitted light and fluorescence channels (excitation at 633 nm and detection between 643 and 700 nm) to check for cell morphology and monitor background signal or uncaging of PENB-DDAO 3, respectively. For one-photon uncaging cells have been irradiated by a 340 to 380 nm monophotonic excitation light for 2 min with a 50W HBO lamp. For two-photon uncaging a delineated cytoplasmic area ($\sim 5 \times 5 \mu\text{m}$) of one cell has been irradiated during 2 s by a 770 nm two-photon laser. The power at the output of the objective was 1 mW. For time-lapse imaging uncaging was performed with a 405 nm-wavelength laser diode focused on a cytoplasmic region of $5 \times 5 \mu\text{m}$ in one cell during 1 s. Z-stacks of $10 \mu\text{m}$ (10 planes with a Z-step of $1 \mu\text{m}$) including the whole cell volume were performed. The power at the output of the objective was around $500 \mu\text{W}$. The fluorescence emission (643–700 nm) and transmitted light were recorded by performing a 4D (X, Y, Z, T) acquisition during 5 min at a frequency of one image every 11 s. A median filter (3×3) is applied to the stacks to smooth the images.

For FRAP-type experiments one-photon uncaging was performed with a HBO lamp, as described above. Then a small region of interest, ROI, (diameter of $5 \mu\text{m}$) in the cytoplasm of one cell was defined. The averaged fluorescence intensity inside this ROI but also in the whole cell and the background were measured during time (1 image every 514 ms during 15 s), before, during, and after photobleaching (photobleaching was performed with the 488, 514, 543, and 633 nm lasers at their maximal power).

For the analysis of the fluorescence recovery curves, each image is background subtracted, corrected for photobleaching, and then normalized according to Phair and Misteli.²³

$$I_{\text{corr}} = \frac{T_0 I_t}{T_t I_0}$$

with T_0 and I_0 being the averaged intensity of the whole cell and the region of bleach, respectively, before photobleaching and where T_t and I_t are the averaged intensity of the same regions during time.

(23) Phair, R. D.; Misteli, T. *Nature* **2000**, 404, 604–609.

To lower or avoid rapid diffusion of the fluorophore, cells (with uncaged fluorophores) were fixed with 4% paraformaldehyde in PBS for 10 min, washed once with HBSS, and then incubated in methanol. Cells were then irradiated (uncaging conditions as above) and a FRAP experiment was performed as for living cells.

Results and Discussion

Synthesis and optical properties. Several reasons prompted the selection of the DDAO chromophore. DDAO is a far-red emitting fluorophore with acceptable brightness ($\epsilon\Phi_f = 3600$ at 658 nm) and surprisingly, despite its fairly simple tricyclic structure, it has been scarcely used in the literature.^{24,25} The presence of a phenol group for which a pK_a around 5.0 has been determined, ensures its complete deprotonation in a neutral biological buffer (pH 7.4). Importantly, the formation of the phenolate is accompanied by a huge shift of its absorbance: from 478 to 645 nm (see pK_a determination in Supporting Information, Figure S1) together with a large enhancement of its fluorescence (not shown). This phenol was therefore targeted for its modification by a photoactivatable group. Scheme 1 shows the transformation of this phenol group into a corresponding ether function using a Mitsunobu coupling reaction with the hydroxyl group of 3-(2-propyl-1-ol)-4'-tris-ethoxy(methoxy)-4-nitrophenyl (2) used as a photoremovable protecting group.²⁶ PENB (2) was prepared using an adapted procedure derived from the synthesis of a 4'-methoxy biphenyl derivative (PMNB),²⁶ the methoxy group of the PMNB derivative being replaced by a more water-soluble tris-ethoxy(methoxy) group.

The caged PENB-DDAO (3a and 3b) was obtained as a $\sim 95/5$ mixture of isomers. Since both isomers are photoactivatable precursors of the same DDAO fluorophore in buffered medium, they were not separated. Importantly, compound(s) 3 can easily be synthesized at larger scale (>100 mg), facilitating

(24) Richard, J.-A.; Meyer, Y.; Jolivet, V.; Massonneau, M.; Dumeunier, R.; Vaudry, D.; Vaudry, H.; Renard, P.-Y.; Romieu, A. *Bioconjugate Chem.* **2008**, 19, 1707–1718.

(25) Bolinger, P.-Y.; Stamou, D.; Vogel, H. *Angew. Chem. Int. Ed.* **2008**, 47, 5544–5549.

(26) Gug, S.; Charon, S.; Specht, A.; Alarcon, K.; Ogden, D.; Zietz, B.; Leonard, J.; Hacke, S.; Bolze, F.; Nicoud, J.-F.; Goeldner, M. *ChemBioChem* **2008**, 9, 1303–1307.

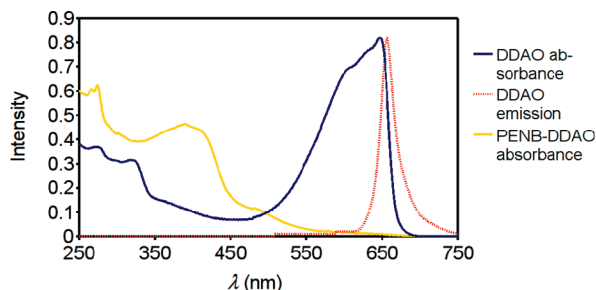


Figure 1. Overlay of PENB-DDAO **3** and DDAO **1** absorbance (concentration = 1.6×10^{-5} M) and DDAO emission (excitation at 600 nm) in acetonitrile/phosphate buffer (pH 7.4) mixture (1:1). Fluorescence emission of PENB-DDAO is not reported because it was not measurable at the same concentration.

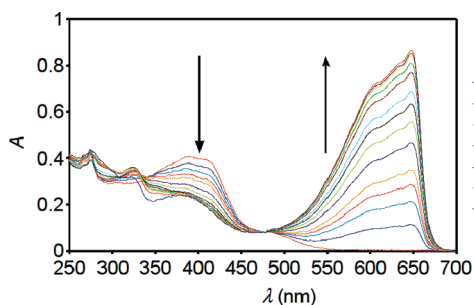


Figure 2. Photolysis of PENB-DDAO **3** in acetonitrile/phosphate buffer (pH 7.4) mixture (1:1). Irradiation at 315 nm.

further chemical modifications of this fluorophore. The structure of **3a** was nonambiguously established as described in the Supporting Information.

Figure 1 displays an overlay of the UV absorption spectra of DDAO **1** and the caged-DDAO **3** as well as the fluorescence emission spectrum of DDAO ($\lambda_{\text{em}} = 658$ nm). Interestingly, the caging group and the fluorophore possess nonoverlapping high absorbance areas, between 300–360 and 590–650 nm, respectively. This leads to an ideal situation where the caged fluorophore can be unmasked ($\lambda_{\text{exc}} < 400$ nm) and concomitantly excited at wavelength ≥ 590 nm for fluorescence imaging without background noise from the remaining caged-DDAO **3**, which is totally nonfluorescent at these wavelengths. In addition, this large absorption area of DDAO will allow efficient fluorescence excitation between 590 and 620 nm avoiding direct fluorescence excitation, and corresponding to a large Stokes-shift. Finally, the sensitivity to photobleaching of the DDAO chromophore is of the same order of magnitude than Rhodamin B (see Supporting Information).

Stability. Contrary to benzylic DDAO ethers, which have been synthesized as pro-fluorophores for penicillin G acylase²⁴ and which were unstable in neutral buffer, the caged fluorophore **3** was fully stable to hydrolysis in the dark in buffered medium at pH 7.4 (no alteration was detected by UV absorbance spectroscopy analysis after 48 h).

One-Photon Photolysis. Quantum Yield Determinations. The photochemical transformation (uncaging) of compound(s) **3** into the DDAO molecule **1** is shown in Figure 2 ($\lambda_{\text{exc}} = 315$ nm). The presence of isosbestic points reveals, at first, a uniform photochemical transformation, analogous to the photolytic transformation of the PMNB-caged glutamate²⁶ while longer irradiation times lead to subsequent evolution of the photolytic reaction. HPLC analysis of the reaction indicates a $\geq 95\%$ conversion into the DDAO chromophore. Finally, the quantum

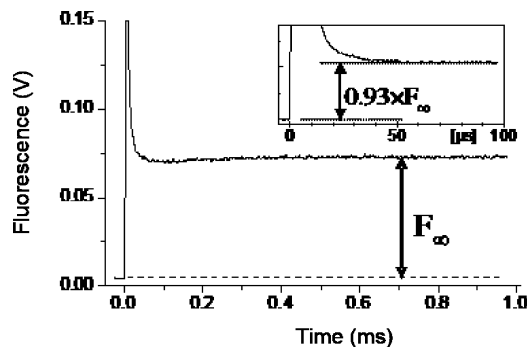


Figure 3. Kinetics of the impulsive photolysis of PENB-DDAO **3** in acetonitrile/phosphate buffer (pH 7.4) mixture (1:1). After a strong initial peak due to the intense photolysis pulse, the asymptotic fluorescence level F_{∞} is reached in less than 0.5 ms. (Inset) Zoom at shorter times: more than 90% of F_{∞} is released in less than 50 μs .

yield of photofragmentation of the PENB-DDAO molecule has been determined using PMNB-Glu²⁶ as a reference and gives a value of $\Phi_u = 0.1$, leading to a high one-photon induced uncaging efficiency ($\epsilon\Phi_u = 1000 \text{ M}^{-1}\cdot\text{cm}^{-1}$ at 365 nm).

Kinetic Measurements. The large spectral shift observed during the uncaging process allowed us, for the first time, to use the detection of the fluorescent signal to monitor the fragmentation kinetics. Uncaging excitation at 355 nm can be accompanied in an independent manner by continuous fluorescence excitation at 590 nm, since the caged compound does not absorb at 590 nm (see Figure 2). Figure 3 shows the detected fluorescent signal as a function of delay time. At time zero, the very large excitation intensity of the photolysis UV pulse generates intense parasitic nanosecond-long emission, which saturates the detector over microseconds. Then, in less than 50 μs a stationary level of fluorescence F_{∞} is reached, which represents 12% of that obtained after complete photolysis of the sample. Most importantly, while the detector is saturated by the initial emission peak (i.e., 40–50 μs after the photolysis pulse, see the inset), more than 90% of F_{∞} is already released. Therefore we conclude that the time constant associated with the dominant process of fluorescence release is shorter than 15 μs . This upper value is in agreement with the reported kinetics for an *o*-nitrophenethyl (DMNPB) caged hydroxycoumarin derivative that was determined by following the absorbance increase at 410 nm after laser flash photolysis.¹⁰

Two-Photon Photolysis. While efficient alcohol two-photon uncaging has been described that leads to the generation of coumarin derivatives as fluorescent reporters,²⁷ direct two-photon fluorophore uncaging has been sparingly described in the literature,^{9,10,15} which focuses on hydroxycoumarin derivatives. The selected PMNB-caging group, composed of a donor/acceptor–biphenyl platform, displayed a remarkable two-photon uncaging cross-section for glutamate release (3.2 and 0.45 GM at 740 and 800 nm, respectively).^{21,26} The two-photon uncaging cross-section $\delta_a\Phi_u$ of the caged-DDAO molecule **3** determination gave values of 3.7 GM at 740 nm. Figure 4 displays the two-photon uncaging cross-section spectrum from 740 to 840 nm and which is ≥ 2 GM from 740 to 780 nm. The two-photon uncaging efficiency is similar to that previously measured for the uncaging of glutamate (PMNB-Glu).^{21,26}

Cell Imaging. Finally, to investigate cellular applications using the PENB-DDAO derivative, we showed its cellular perme-

(27) Gagey, N.; Neveu, P.; Benbrahim, C.; Goetz, B.; Aujard, I.; Baudin, J.-B.; Jullien, L. *J. Am. Chem. Soc.* **2007**, *129*, 9986–9998.

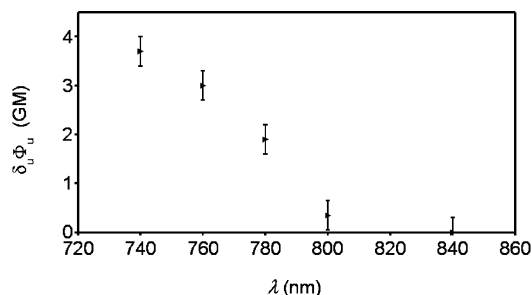
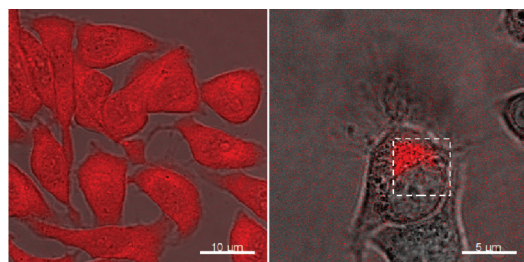


Figure 4. Two-photon uncaging action cross-section ($\delta_a\Phi_u$) of PENB-DDAO **3**.



5a. One-photon irradiation. **5b.** Two-photon irradiation.

Figure 5. Overlay of transmitted light and fluorescence after incubation of HeLa cells with 19.5 μM PENB-DDAO for 30 min and irradiation by a 340–380 nm one-photon excitation (a) or a 770 nm two-photon excitation (b). Irradiation area $\approx 5 \mu\text{m} \times 5 \mu\text{m}$. Fluorescence: excitation at 633 nm, recording between 643 and 700 nm.

ability on HeLa cells and the triggering of a cytoplasmic red fluorescent signal after either monophoton excitation in the range of 340–380 nm (Figure 5a) or two-photon excitation at 770 nm of a delineated area of one cell (Figure 5b). Moreover, it is worthwhile to notice that although the two-photon irradiation area (dotted square in Figure 5b) encompasses part of the nucleus, there is no resulting fluorescence in the nucleus. This suggests that either the PENB-DDAO derivative, in the time frame of the experiment, does not penetrate the nucleus or that fluorescence is quenched within the nucleus.

To assess cellular diffusion of the released fluorophore, we initially performed time-lapse experiments which showed an instant disappearance of the fluorescent signal (Supporting Information, Figure S6). However, considering the time resolution of a Z-scan analysis, we were not able to track the fluorescent signal (not shown). Although in agreement with a freely diffusing cellular species, like a small unbound fluorophore, we decided to perform FRAP-type experiments to establish unambiguously a cellular diffusion process. After photobleaching of a small cytoplasmic area, we could clearly establish a fast and almost full recovery of the fluorescent signal on living cells, while similar experiments performed on fixed

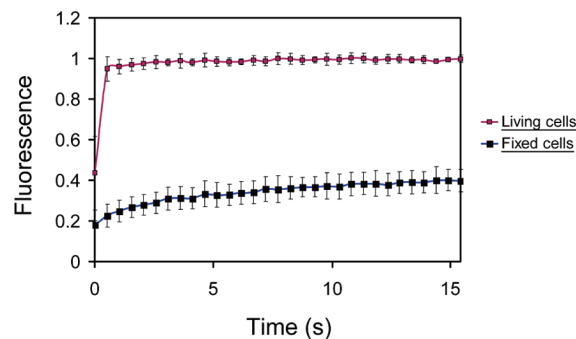


Figure 6. Fluorescence recovery after photobleaching on fixed cells (blue) and living cells (red).

cells showed only a scarce recovery (Figure 6). Clearly, the photoliberated fluorophore diffuses freely and rapidly within the cytoplasm rather than sticking to the membrane or to cellular compartments.

Control figures showing fluorescence and transmitted light before irradiation and time-lapse imaging are available in the Supporting Information, Figures S4, S5, and S6. Importantly, this experiment demonstrates for the first time the possibility to turn on a fluorescent signal in a precise area of a single cell using a caged fluorophore.

Conclusions

We describe here the total synthesis of a photoactivatable acridinone derivative (PENB-DDAO **3**), which upon photolysis rapidly (μs time-range) and efficiently ($\geq 95\%$), releases 1,3-dichloro-9,9-dimethyl-9H-acridin-2(7)-one (DDAO), a far-red emitting fluorophore. PENB-DDAO is the first caged fluorophore to encompass both very high two-photon sensitivity (uncaging cross section $\delta_a\Phi_u \geq 3.7 \text{ GM}$ at 740 nm) and far-red emission wavelength requirements ($\lambda_{\text{em}} = 658 \text{ nm}$). Two-photon triggering of a red fluorescent signal in HeLa cells represents promising preliminary results for potentially sophisticated dynamic live-cell imaging studies.

Acknowledgment. The authors thank Dr. Pascal Didier and Prof. Yves Mely for two-photon irradiations, we thank Aline Huber for technical assistance, the ANR (Contract No. PCV 07 1-0035), the CNRS, the French Ministry of Research, and the Université de Strasbourg for financial support.

Supporting Information Available: Solvent preparation, HPLC methods, determination of the structure of PENB-DDAO **3a** and **3b**, pK_a determination of DDAO, aqueous solubility assays, comparative bleaching experiments, control figures for live-cell imaging, time-lapse microscopy figure. This material is available free of charge via the Internet at <http://pubs.acs.org>.

JA9074562